

Superprism phenomena in polymeric woodpile structures

Jesper Serbin^{a)} and Min Gu^{b)}

Centre for Micro-Photonics and Centre for Ultra-High Bandwidth Devices for Optical Systems (CUDOS),
Faculty of Engineering and Industrial Science, Swinburne University of Technology, P.O. Box 218,
Hawthorn, Victoria 3122, Australia

(Received 15 April 2005; accepted 9 November 2005; published online 27 December 2005)

An analysis of the optical properties of photonic woodpile structures is presented. We demonstrate large superprism phenomena inside polymeric woodpile structures having a refractive index of less than $n=1.6$. Due to the low contrast in refractive indices the structures investigated do not possess a complete photonic band gap. Nevertheless, their photonic band structures show strong anisotropy at frequencies slightly above the band gap in the (Γ - X) direction, leading to an extreme sensitivity to the angle and the frequency of the incident light in the propagation direction inside the crystal. Furthermore, if the woodpile structure is arranged in a prism-like shape, the transmitted beam outside the crystal shows a strong sensitivity to the frequency and angle of the incident light.

© 2005 American Institute of Physics. [DOI: 10.1063/1.2149163]

I. INTRODUCTION

Recently the fabrication of woodpile structures having a photonic band gap in the near-infrared wavelength region by means of two-photon polymerization has been reported by several groups.¹⁻⁷ Since the applied polymers have a refractive index of only $n=1.47$ (Ormocer's⁸) to $n=1.56$ (Ormocer's⁸ and SU8⁵), the structures demonstrated only possess photonic band gaps (PBG's) in certain directions. This technique cannot be utilized for the fabrication of complete PBG materials. Nevertheless, our simulations show that even in the absence of a complete PBG, the woodpile structure possesses extremely strong superprism properties. There have been several studies on the propagation properties of photonic crystals. Most of these investigations were carried out for two-dimensional lattices⁹⁻¹¹ and only very few publications can be found on three-dimensional (3D) crystals.¹² To calculate the propagation properties inside the woodpile structures we chose a method that was first suggested by Kosaka *et al.*,^{13,14} utilizing the complete photonic band structure. The calculations of the band structures shown within this work have been performed by means of the freely available software package MPB (Ref. 15) utilizing the plane wave method.

II. THE WOODPILE STRUCTURE

A sketch of a woodpile structure is shown in Fig. 1. The crystal consists of layers of one-dimensional rods with a stacking sequence that repeats itself every four layers. The distance between four adjacent layers is denoted by c . Within each layer, the axes of the rods are parallel to each other with a distance d between them. The adjacent layers are rotated by 90° . Between every other layer, the rods are shifted relative to each other by $d/2$. Generally, the resulting structure has a face-centered-tetragonal (fct) lattice symmetry. For the special case of $c/d=\sqrt{2}$, the lattice can be derived from a face-

centered-cubic (fcc) unit cell with the basis of two rods.¹⁶ The following calculations all were accomplished for crystals having fcc symmetry.

III. COMPLETE BAND STRUCTURES OF POLYMERIC WOODPILE STRUCTURES

Figure 2 shows the calculated band structure for a woodpile structure having a contrast in the refractive index of $n=1.47$. The rods of the respective structure have an elliptical cross section. The width and the height of the rods are $w=0.3d$ and $h=0.7d$, respectively, where d is the in-layer rod spacing (see Fig. 1, top). The band structure is shown for a path along high symmetry points within the irreducible Brillouin zone.

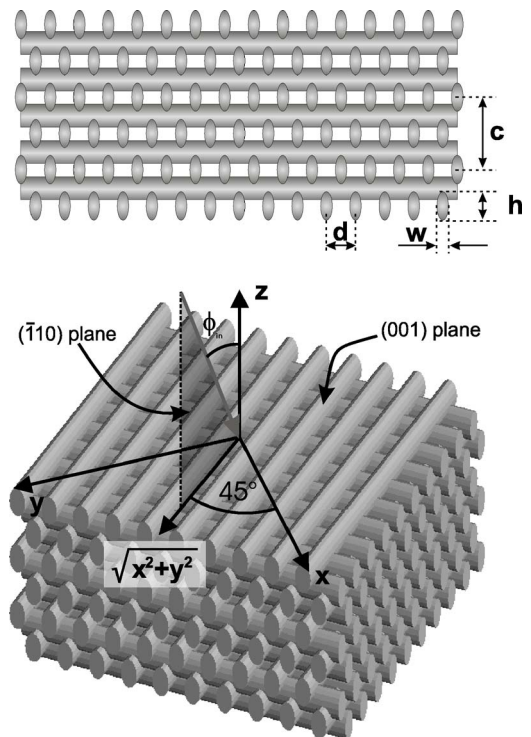


FIG. 1. Sketch of a woodpile structure showing the planes investigated and the woodpile dimensions.

^{a)}Electronic mail: jserbin@swin.edu.au

^{b)}Electronic mail: mgu@swin.edu.au

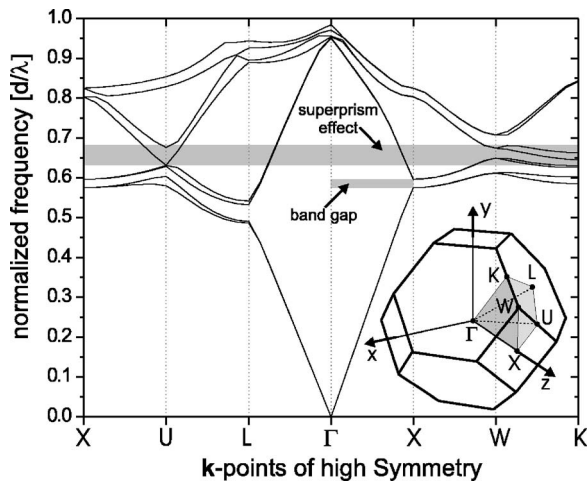


FIG. 2. Photonic band structure of a woodpile having a contrast in a refractive index of 1.47 (the frequencies are in units of d/λ).

loun zone (see the lower right corner of Fig. 2). Due to the low contrast in refractive index these woodpile crystals do not possess a complete PBG. However, there is a band gap in the (Γ - X) direction at a normalized frequency of $\omega=0.585$ (ω in terms of d/λ) with a gap to mid-gap ratio of 3.6%. To determine the propagation properties inside the woodpile structure, the complete photonic band structure has to be calculated (i.e., the modes for all k vectors that are within the irreducible Brillouin zone) rather than only for the path along high symmetry points. To do this, the surface of the irreducible Brillouin zone was divided into three triangles (determined by the high symmetry points (X - U - W , L - U - W , and L - K - W), and each of these triangles was divided into 861 k points (the number of k points determines the resolution of the following calculations), representing the respective directions. The band structure was calculated for k vectors directing from the Γ point to the respective k value within the triangles. For each direction, the magnitude of the k vectors was varied in steps of $|k|_{\max}/30$. In more simple fcc crystals like the artificial opal, where the primitive lattice cell only contains one single sphere at the origin, the surface of the entire Brillouin zone can be described by one set of such three triangles due to symmetry properties. Since the primitive cell of a woodpile structure is based on two perpendicular rods, not all of those symmetry conditions are valid anymore, and to cover the entire surface of the Brillouin zone, the calculations have to be carried out for three sets of triangles (i.e., $[XUW, LUW, LKW]$, $[X'U'W', LU'W', LKW']$, and $[X'U'W'', LU'W'', LK'W'']$; see Fig. 3).

This allows us to determine $\omega(\mathbf{k})$ for all values of \mathbf{k} within the Brillouin zone. To understand the refraction properties of the woodpile structure it is useful to determine $\mathbf{k}(\omega)$, which is the inverse problem. To solve this, $\omega(\mathbf{k})$ was inverted numerically, allowing us to calculate the iso energy surfaces (IESs) $\mathbf{k}(\omega)$ for fixed frequencies ω .

The IESs for a woodpile structure having a contrast in the refractive index of $\Delta n=1.47$ are shown in Fig. 4 for normalized frequencies of $\omega=0.40$ (second band) and $\omega=0.68$ (fourth band). As one would expect, the woodpile structure behaves like a homogeneous medium with an ef-

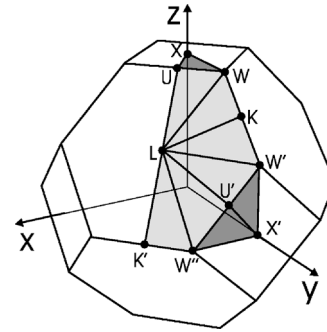


FIG. 3. Brillouin zone of a fcc lattice and the points of high symmetry taken into account for the calculation of the complete band structure.

fective refractive index for frequencies far below the band gap, leading to a spherical-shaped IES (the left image in Fig. 4). The radius of the sphere, which determines the magnitude of the wave vector, is $|\mathbf{k}|=0.676$, which corresponds to a group velocity of $|\mathbf{v}_{\text{group}}|=c/n_{\text{eff}}$. For frequencies slightly above the band gap, the strong anisotropy of the dispersion relation, which leads to a star-like shape of the IES, becomes obvious (the right image in Fig. 4). Since the direction of the group velocity (as well as the direction of energy flow) of the propagating light are determined by the gradient of ω with respect to \mathbf{k} ($\nabla_{\mathbf{k}}\omega$), the surface normals of the IES determine the propagation direction inside the photonic crystal¹⁴ and generally point to another direction as the respective \mathbf{k} vector leading to the superprism phenomenon.¹⁷ These internal propagation properties will be investigated in a more detailed way in the following section.

IV. PROPAGATION INSIDE THE WOODPILE STRUCTURE

The following calculations were performed for light incident to the (001) plane of the woodpile structure (see Fig. 1, lower image) at an azimuth angle of $\theta=45^\circ$. Due to the conservation of the parallel component of the k vector at the transition from one medium to another, the light inside the crystal will be confined to the ($\bar{1}10$) plane, as indicated in the sketch, i.e., the parallel component k_{\parallel} points in the direction of the rods and the normal component k_{\perp} points in the stacking direction. In the following the propagation inside the crystal will be investigated as a function of the elevation angle ϕ and the normalized frequency ω .

Figure 5 shows the internal propagation angle ϕ_{prop} as a function of the normalized frequency for different angles of incidence. The shown simulations were performed with a contrast in a refractive index of 1.47. To obtain ϕ_{prop} the wave vectors \mathbf{k} for the propagating light were calculated numerically utilizing the complete photonic band structure, taking the conservation of the parallel component into account. Subsequently, the direction of propagation was obtained by determining the vector normal to the IES at the respective \mathbf{k} point. For frequencies slightly above the band gap, the woodpile structure shows negative refraction ($\phi_{\text{prop}} \approx -11^\circ$), a phenomenon that has recently been discussed by several groups.¹⁸⁻²⁰ With increasing frequency, the propagating angles show a shift to positive values of $\phi_{\text{prop}} \approx 79^\circ$. The

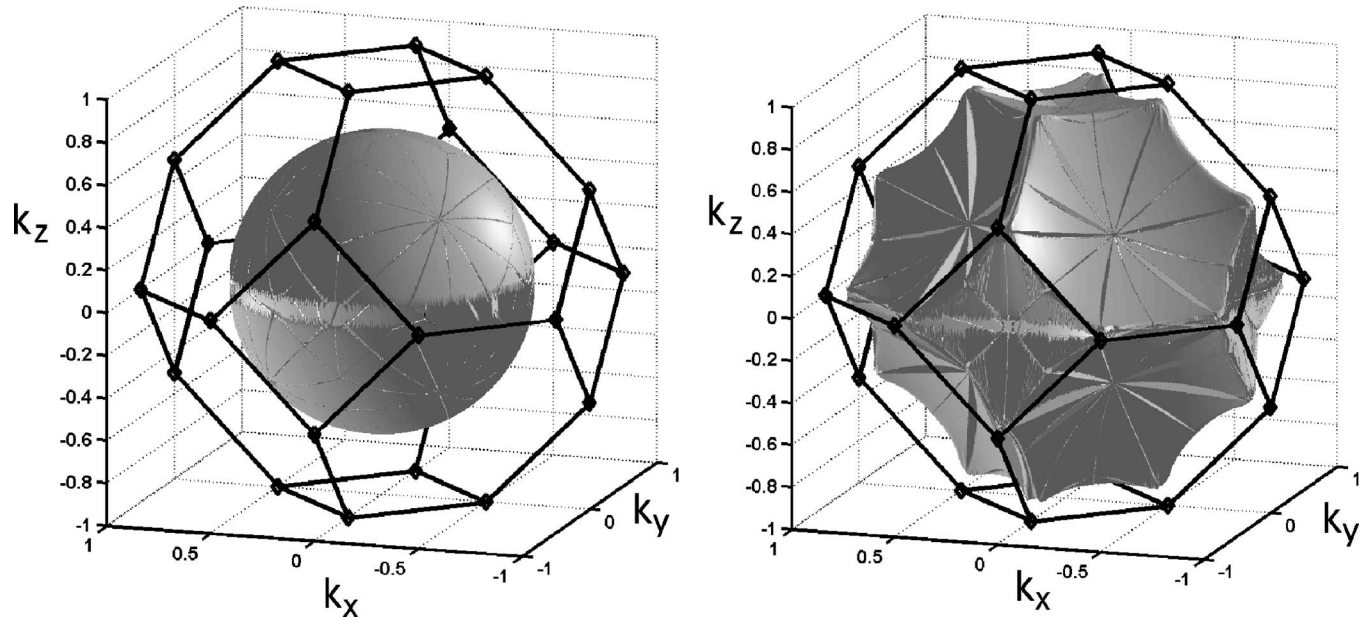


FIG. 4. Isoenergy surfaces (IESs) of a woodpile structure with a refractive index of $n=1.47$. The plots show the IESs at a normalized frequency of $\omega=0.40$ (left) and $\omega=0.68$ (right) within the second and fourth bands, respectively.

frequency of high sensitivity varies with the angle of the incident light, as shown for $\phi_{in}=21^\circ$ to 25° . These values are of the same order as reported for inverted artificial opal structures.²¹

It has been demonstrated that woodpile structures for the near infrared can be fabricated by means of two-photon polymerization of hybrid polymers (*ORMOCERS*⁷), which have a refractive index that can be tuned by means of chemical design between $n=1.47$ and $n=1.56$. Figure 6 shows how the frequency of high sensitivity changes with a variation of the refractive index within those values. Although the gap to mid-gap ratio of the PBG decreases from 4.7% to 3.6% when changing the refractive index from $n=1.56$ to $n=1.47$, the change in magnitude of the angular shift is negligible.

All of the data shown were calculated in terms of normalized frequencies $\omega=d/\lambda$. It has been demonstrated by

several groups that woodpile structures can be fabricated by means of two-photon polymerization with in-layer rod distances of $1\ \mu\text{m}$ and below,⁵⁻⁷ which would lead to strong superprism effects at wavelengths of about $1.5\ \mu\text{m}$. A woodpile structure having an in-layer rod distance of $d=0.8\ \mu\text{m}$, for example, would exhibit a shift in the propagation angle from $\phi_{prop}\approx -11^\circ$ to $\phi_{prop}\approx 78^\circ$ within a range of wavelengths reaching from $\lambda\approx 1.55\ \mu\text{m}$ to $\lambda\approx 1.50\ \mu\text{m}$ at an incident angle of $\phi_{in}=22^\circ$. This corresponds to a sensitivity of $17.8^\circ/\text{nm}$.

V. PROPAGATION OUTSIDE THE WOODPILE STRUCTURE

In the previous section, the propagation of light inside the woodpile structure has been discussed and strong sensi-

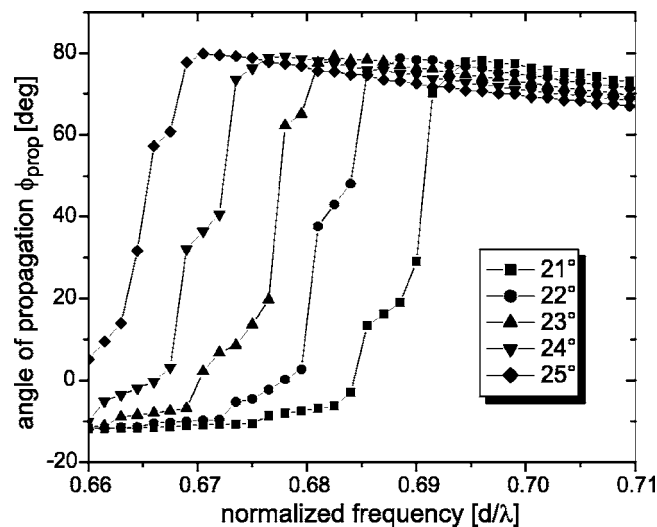


FIG. 5. Internal propagation angle ϕ_{prop} as a function of the normalized frequency for different angles of incidence $\phi_{in}=21^\circ, 22^\circ, 23^\circ, 24^\circ,$ and 25° .

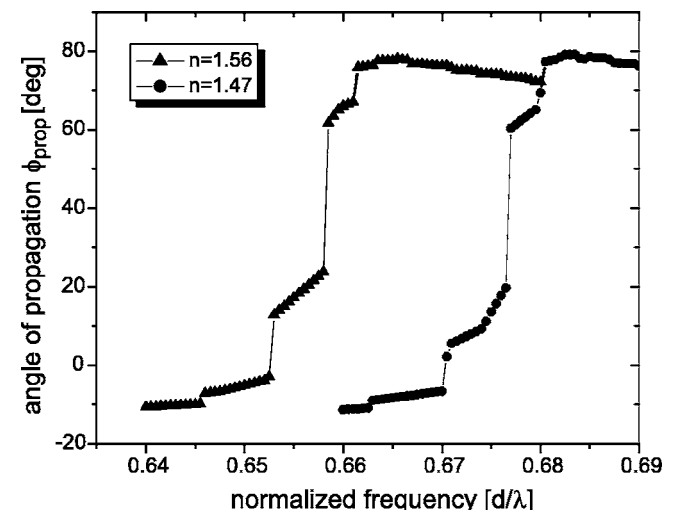


FIG. 6. Internal angle of propagation for light incident at $\phi_{in}=30^\circ$ as a function of the normalized frequency. A change in the refractive index from $n=1.47$ to $n=1.56$ causes a shift in the frequency of high sensitivity from $\omega=0.658$ to $\omega=0.677$.

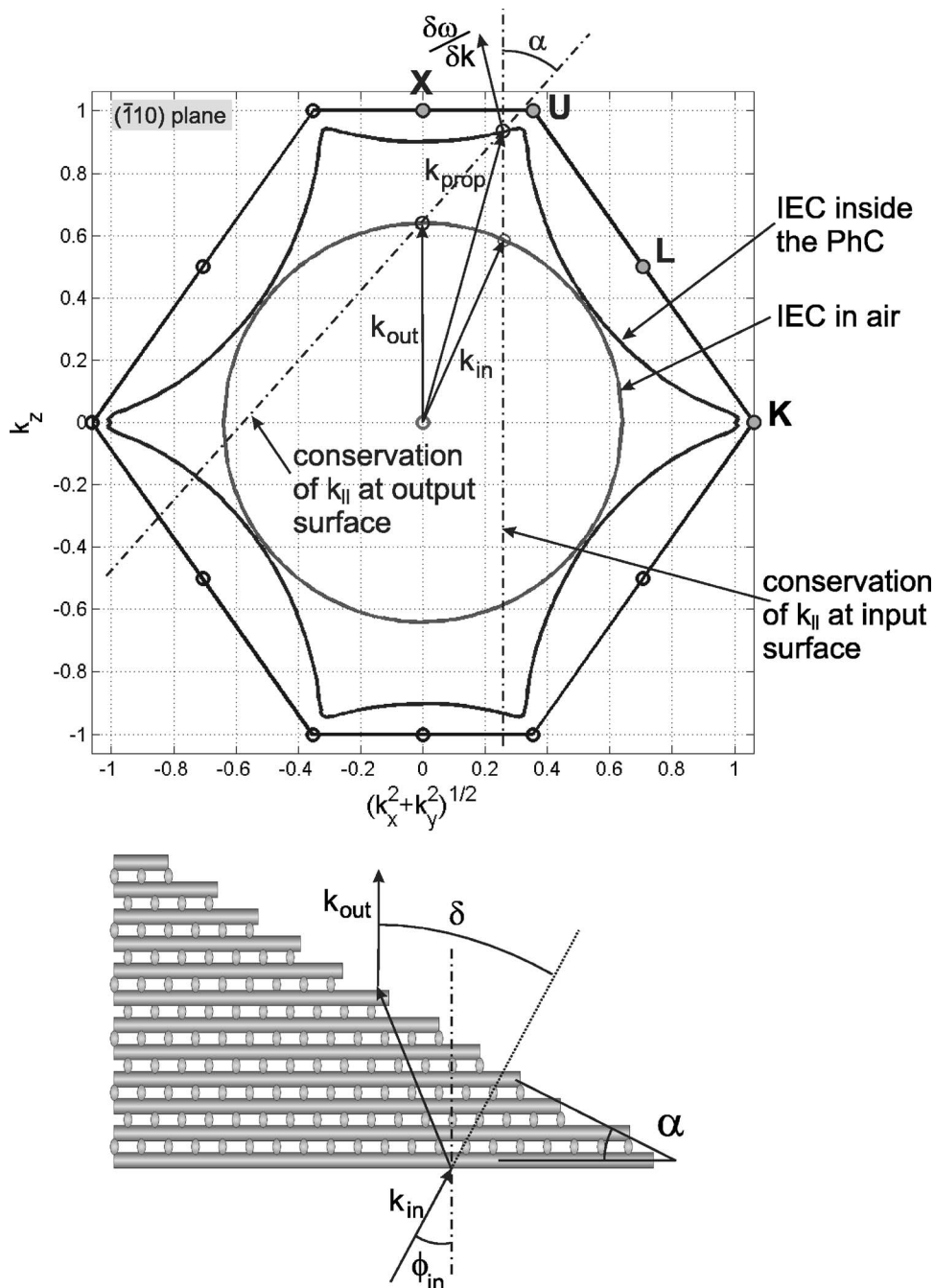


FIG. 7. Isoenergy contour [intersection of the IES with the $(\bar{1}10)$ plane] for a polymeric woodpile structure at a normalized frequency of $\omega=0.64$ and a sketch of a woodpile prism.

tivity of the propagating angles on the frequency and the angle of incidence has been observed. However, from the experimental side of view, the light that is transmitted by the photonic crystal structure is much more easily accessible than the light inside the crystal. The propagation direction of the transmitted light can be derived in the same manner as the light inside the crystal, with the only difference that two tilted interfaces have to be considered now.

Figure 7 shows schematically how the direction of the transmitted light can be determined for a woodpile prism with an opening angle α . The plot shows an isoenergy contour (IEC) for a $(\bar{1}10)$ plane in the woodpile structure ($\theta = 45^\circ$). This plane is defined by the z axis and the bisector of

the x - y plane ($\sqrt{k_x^2 + k_y^2}$). The k vector for the light propagating inside the crystal k_{prop} is determined by the intersection of the vertical (dash-dotted) line and the IEC, leading to conservation of $k_{||}$. To obtain the k vector and hence the direction of propagation outside the crystal one has to take the conservation of $k_{||}$ into account, this time with respect to the second interface that is tilted by an angle of α , leading to k_{out} . The output angle ϕ_{out} will be treated as the angle between \mathbf{k}_{out} and the normal to the input surface (rather than the output surface).

Due to this construction scheme, it is obvious that the direction of propagation outside the crystal is independent of the propagation direction inside the crystal, since only \mathbf{k} vec-

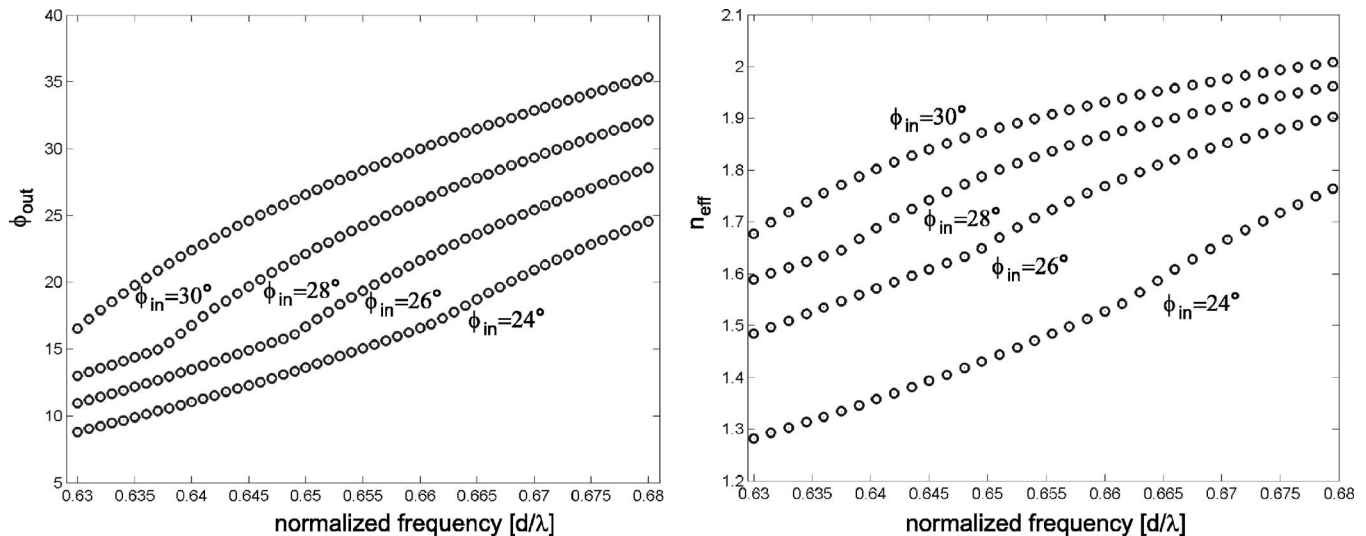


FIG. 8. (Left) Angles of the output beam as a function of the normalized frequency for different incident angles. (Right) Effective refractive indices derived from Snell's law as a function of the normalized frequency.

tors are taken into account, but not the group velocity $\partial\omega/\partial\mathbf{k}$ of the propagating light. Hence, strong effects such as negative refraction cannot be observed outside the crystal. Nevertheless, a strong sensitivity of the propagating angle of the output beam on the frequency was observed. ϕ_{out} swings from 16° to 35° as the frequencies are varied between $\omega = 0.63$ and $\omega = 0.68$ at an incident angle of $\phi_{in} = 30^\circ$, which corresponds to an average sensitivity of $0.16^\circ/\text{nm}$.

By fitting the calculated data for $\phi_{out} = \phi_{out}(\omega, \alpha, \phi_{in})$ to Eq. (1), which was derived by applying Snell's law and solving the equation for n_{eff} , one obtains an effective refractive index for the considered woodpile structure:

$$\delta = \sin^{-1}[(\sin \alpha)(n_{eff}^2 - \sin^2 \phi_{in})^{1/2} - \sin \phi_{in} \cos \alpha] + \phi_{in} - \alpha, \quad (1)$$

where δ is the angle between the input and the output beam.

This dependence is shown in Fig. 8 for different angles of incidence. An increase of up to 30% of the effective refractive index can be observed when tuning the frequency of the incident light from $\omega = 0.63$ to $\omega = 0.68$.

VI. CONCLUSION

We have demonstrated strong superprism effects inside photonic woodpile structures at frequencies slightly above the band gap. The calculations were performed for structures that have already been realized by several groups, with the main intention of fabricating PBG structures. We have investigated the propagation properties of these structures theoretically. The angles of the light propagating inside woodpile structures is very sensitive to the frequency and the angle of incidence. A sensitivity of up to $17.8^\circ/\text{nm}$ at a wavelength of $\lambda \approx 1.5 \mu\text{m}$ for a photonic crystal with an in-layer rod spacing of $1 \mu\text{m}$ was shown. If the woodpile structure is designed in a prism-like shape, superprism effects can also be observed outside the woodpile structure with a sensitivity of $0.16^\circ/\text{nm}$. Since two-photon polymerization is a truly 3D direct laser writing method, it is straightforward to fabricate woodpile structures of arbitrary prism shapes and also to

integrate them into 3D waveguide structures. This opens a wide field of applications for very compact devices such as dense wavelength division multiplexers.

ACKNOWLEDGMENT

This work was produced with the assistance of the Australian Research Council under the ARC Centres of Excellence program. CUDOS (the Centre for Ultrahigh-Bandwidth Devices for Optical Systems) is an ARC Centre of Excellence.

- ¹S. Maruo, O. Nakamura, and S. Kawata, *Opt. Lett.* **22**, 132 (1997).
- ²B. H. Cumpston, S. P. Ananthavel, S. Barlow, D. L. Dyer, J. E. Ehrlich, L. L. Erskine, A. A. Heikal, S. M. Kuebler, I.-Y. S. Lee, D. McCord-Maughon *et al.*, *Nature (London)* **398**, 51 (1999).
- ³H.-B. Sun, S. Matsuo, and H. Misawa, *Appl. Phys. Lett.* **74**, 786 (1999).
- ⁴H.-B. Sun, V. Mizeikis, Y. Xu, S. Juodkakis, J.-Y. Ye, S. Matsuo, and H. Misawa, *Appl. Phys. Lett.* **79**, 1 (2001).
- ⁵M. Deubel, G. V. Freymann, M. Wegener, S. Pereira, K. Busch, and C. Soukoulis, *Nat. Mater.* **3**, 444 (2004).
- ⁶M. Straub and M. Gu, *Opt. Lett.* **27**, 1824 (2002).
- ⁷J. Serbin, A. Ovsianikov, and B. Chichkov, *Opt. Express* **12**, 5221 (2004).
- ⁸J. Serbin, A. Egbert, A. Ostendorf, B. N. Chichkov, R. Houbertz, G. Domann, J. Schulz, C. Cronauer, L. Fröhlich, and M. Popall, *Opt. Lett.* **28**, 301 (2003).
- ⁹L. Wu, M. Mazilu, T. Karle, and T. F. Krauss, *IEEE J. Quantum Electron.* **38**, 915 (2002).
- ¹⁰S.-Y. Lin, V. M. Hietala, L. Wang, and E. D. Jones, *Opt. Lett.* **21**, 1771 (1996).
- ¹¹J. Bravo-Abad, T. Ochiai, and J. Sanchez-Dehesa, *Phys. Rev. B* **67**, 115116 (2003).
- ¹²T. Ochiai and J. Sanchez-Dehesa, *Phys. Rev. B* **64**, 245113 (2001).
- ¹³H. Kosaka, T. Kawashima, A. Tomita, M. Notomi, T. Tamamura, T. Sato, and S. Kawakami, *Phys. Rev. B* **58**, R10 096 (1998).
- ¹⁴H. Kosaka, T. Kawashima, A. Tomita, M. Notomi, T. Tamamura, T. Sato, and S. Kawakami, *J. Lightwave Technol.* **17**, 2032 (1999).
- ¹⁵S. G. Johnson and J. D. Joannopoulos, <http://ab-initio.mit.edu/mpb> (1999).
- ¹⁶S. Lin, J. Fleming, D. Hetherington, B. Smith, R. Biswas, K. Ho, M. Sigalas, W. Zubrzycki, S. Kurtz, and J. Bur, *Nature (London)* **394**, 251 (1998).
- ¹⁷K. Sakoda, *Optical Properties of Photonic Crystals* (Springer, Berlin, 2001).
- ¹⁸J. B. Pendry, *Phys. Rev. Lett.* **85**, 3966 (2000).
- ¹⁹R. A. Shelby, D. R. Smith, and S. Schultz, *Science* **292**, 77 (2001).
- ²⁰Z. M. Zhang and C. J. Fu, *Appl. Phys. Lett.* **80**, 1097 (2002).
- ²¹T. Prasad, V. Colvin, and D. Mittleman, *Phys. Rev. B* **67**, 165103 (2003).